

# Refractory Characteristics of Aluminum Dross-Kaolin Composite

S.O. ADEOSUN,<sup>1,3</sup> E.I. AKPAN,<sup>2,4</sup> and M.O. DADA<sup>1,5</sup>

1.—Department of Metallurgical and Materials Engineering, University of Lagos, Lagos, Nigeria. 2.—Department of Materials and Production Engineering, Ambrose Alli University, Ekpoma, Edo State, Nigeria. 3.—e-mail: samsonoluropo@yahoo.com. 4.—e-mail: emma\_eia@yahoo.com. 5.—e-mail: modupeoladada@gmail.com

The suitability of using aluminum dross waste and kaolin to produce refractory bricks is experimentally studied. Thirty brick samples of different blends are produced, dried at 30°C, dried further at 110°C, and fired at 1200°C. The firing temperature point, bulk density, apparent porosity, thermal conductivity, thermal shock, loss on ignition, permeability, shatter index, and shrinkage of the bricks blends are determined. The results show that some blend samples have good refractory characteristics with mixing ratio 4:1:2 (representing weight in grams of aluminum dross, plastic clay, and kaolin, respectively). The evaluations of studied properties reveal the possibility for aluminum dross waste to be used as matrix in refractory bricks.

## INTRODUCTION

Refractories are heat-resistant materials used in almost all processes involving high temperatures and/or corrosive environments. These are typically used to insulate and protect industrial furnaces and vessels because of their excellent resistance to heat and mechanical damage.<sup>1</sup> Refractory materials can be made from clay and nonclay refractory. Nonclay refractory are made of alumina, zirconia, silicon carbide, chromia, magnesite, graphite, and other less common materials, but the cost of the nonclay refractory is much higher than that of fire clay.<sup>2</sup> The various combinations of operating conditions, in which refractories are used, make it necessary to manufacture a range of refractory materials with different properties.

Aluminum dross is a by-product of aluminum production. Forms of dross are white, black, and salt cake.<sup>3</sup> White dross is formed during the primary Al refining process, whereas black dross and salt cake are formed during the secondary refining process in which large amounts of chloride salt fluxes are used. The main constituents of dross are Al and Al<sub>2</sub>O<sub>3</sub> with other constituents such as MgO and MgAl<sub>2</sub>O<sub>4</sub>. Primary Al dross contains approximately 80% Al and secondary ones contain approximately 5–10%. Although primary Al dross can be recycled, secondary dross is what is frequently disposed at

landfill sites. Secondary dross contains various compounds in addition to Al. The commonly found compounds are Al<sub>2</sub>O<sub>3</sub> (50–65%), aluminum nitride (AlN, 15–30%), Al (3–5%), MgO (5–10%), SiO<sub>2</sub> (1–2%), CaF (<2%), and other trace salts such as AlP and Al<sub>2</sub>S<sub>3</sub>.<sup>4</sup>

Serious medical conditions associated with Al dross exposure include cancer, liver damage, skin rashes, and reproductive disorders. When deposited and stored in landfills, dross is toxic to the environment as it emits foul, often toxic odors.<sup>5</sup> It is sad to note that no effective and economical technique for reducing the malodorous gas emitted from the stored and disposed dross exists on a large scale.<sup>6</sup>

Recovery of aluminum metal from wastes dross is energy demanding, which could be saved if the dross is diverted and used as an engineering material. The reuse of dross has been examined in view of transforming Al dross into a useful resource. Ewais et al.<sup>7</sup> used varying ratios of Al sludge, Al dross, and Al sinters to manufacture calcium aluminate cement that can be used to produce resistant bricks. In another study, dross is used to produce hexagonal mesoporous aluminophosphate.<sup>8</sup> Hong et al.<sup>9</sup> recycled Al through a submerged and an electric arc furnace to produce an Al–Si alloy and brown-fused alumina, respectively. Yoshimura et al.<sup>10</sup> also used an electrical plasma furnace to process Al dross to be used as an alternative raw material for produc-

ing refractory materials. The study shows that Al dross waste from plasma processing can be applied directly, without prior calcinations, as a fine structural component in castables and pressed refractory material. Other researchers used mixed dross and zircon to prepare mullite/zirconia composites, employing various temperatures and furnace times.<sup>11</sup> Chen's<sup>12</sup> study on the development of Al dross-based material for engineering application tried to eliminate waste and use the waste in a natural closed-loop cycle. Three avenues are investigated to use the dross, which are (I) refractory materials, (II) Al composites, and (III) high-temperature additive for desulfurizing steel. The results indicate that dross can be applied either through a simple purification process or directly as a substitute for fine structural components in refractories. Although pores and defects could be generated from gas releasing reactions, the properties are found acceptable. Lorber and Antrekowitsch's<sup>13</sup> study on the treatment and disposal of residues from Al dross recovery stated that calcination of oxidic residues is a promising technology to convert a waste into a value-added product.

As stated earlier, the major component of aluminum dross is alumina ( $\text{Al}_2\text{O}_3$ , 50–65%), which is the primary ingredient for a significant portion of the refractory products used in high-temperature industrial applications such as metallurgical, cement, ceramic, glass, and petrochemical manufacturing processes.<sup>14</sup> World consumptions of calcined refractory-grade bauxite are about 1 million tons per year and the consumptions of calcined alumina for use in refractory applications is about 500,000 metric tons per year.<sup>15</sup> Thus, dross presents a potential market for alternative alumina source for refractory aggregates.

In the quest for a low-cost recycling procedure for Al dross usage, this study examines the potential of Al dross/kaolin blend as a healthy refractory material in furnaces.

## EXPERIMENTAL METHODOLOGY

### Materials and Methods

The kaolin used for this study was sourced from Ota-Abeokuta west and the Al dross was obtained from Aluminum Rolling Mills (Ota, Ogun state, Nigeria). Kaolin and Al dross were crushed and ground separately, and the powder was sieved using a 5-in diameter perforated plate and sieve set (Model: H-3902) into 150, 212, 300, 425, 500, and 600  $\mu\text{m}$  sizes. Measurement was done using a Model YP30001, 3000-g digital weighing scale in the Al dross:slip:kaolin ratio to give 100 g of the composite blend, and each mix was stored in polythene bag. The measured materials are wet mixed until a satisfactory even distribution of aggregates is achieved. A fabricated wooden-brick mold of dimensions 230  $\times$  113  $\times$  25 mm were made and molding was carried out manually. The dry ingredients were mixed evenly with a constant

amount of slip to form a viscous solution. The mixture was thoroughly mixed and piled to avoid evaporation and drying. The wetting process or tempering was done to allow physical and chemical changes to take place in the blends while improving the molding characteristics. The molded bricks together with their test specimens are air dried at ambient temperature (30°C). The bricks and test specimens are dried in a mechanical (controlled humidity) oven dryer at 110°C. This increases the green strength and allows safe handling for subsequent processing. The dried bricks and test specimens are finally fired to a temperature of 1200°C in an electric kiln. The bricks are fired with the standing rule of one finger space between them to enhance distribution of heat in the kiln. The firing of the bricks is done for 4 h and the kiln with its content turned off to allow soaking period for 1 h before the kiln is opened up and the bricks are brought out. This promotes melting of some constituents of the Al dross resulting in the formation of pores in the finished bricks. The initial/original length, dried length, fired length, wet weight, and dry weights are noted.

## CHARACTERIZATION

### Shrinkage Test

Test specimens from each blend were dried at room temperature (30°C) for more than 14 days to ensure total water loss. The test specimens' dimensions were measured again after the oven drying process and the dry lengths were recorded. After firing at 1200°C, the specimens were allowed to cool and the new weights and dimensions were recorded. The dried, fired, and the total shrinkages were calculated for each test specimen using the following formulas:

$$\text{Average Drying Shrinkage (\%)} = \frac{(\text{OL} - \text{DL})}{\text{OL}} \times 100 \quad (1)$$

$$\text{Average Firing Shrinkage (\%)} = \frac{(\text{DL} - \text{FL})}{\text{FL}} \times 100 \quad (2)$$

$$\text{Total Shrinkage (\%)} = \frac{(\text{OL} - \text{FL})}{\text{OL}} \times 100 \quad (3)$$

where OL is the original length, DL stands is the dry length, and FL is the fired length.

### Apparent Porosity Tests

$$\text{Apparent Porosity (\%)} = \frac{(W - D)}{(W - S)} \times 100 \quad (4)$$

where  $W$  is the weights of soaked specimen suspended in air,  $D$  is the weight of fired specimen, and

$S$  is the weight of fired specimen suspended in water.

### Bulk Density, Apparent Density Test

The test specimens were dried to ensure total water loss and later were fired up to approximately 1200°C in an electric kiln. The cooled and the fired weights were then recorded. These were then immersed in a beaker of water, and the bubbles were observed as the pores in the specimens filled with water. The soaked weights of the specimens were recorded. The specimens were then suspended in a beaker after the other using a sling and the suspended weights were determined.

The bulk density, apparent density, and apparent porosity are calculated using the formula:

$$\text{Bulk Density (g/cm}^3\text{)} = \frac{D}{(W - S)} \times 100 \quad (5)$$

$$\text{Apparent Density (g/cm}^3\text{)} = \frac{D}{(D - S)} \times 100 \quad (6)$$

where  $D$  is the weight of fired specimen,  $S$  is the weight of the fired specimen suspended in water, and  $W$  is the weight of soaked specimen suspended in air.

### Effective Moisture Content Test

The wet brick samples were weighed one after the other, and their weights were recorded. These were dried at 110°C to expel all water molecules, and the dry weights were recorded. The effective moisture content for the brick samples was calculated using the formula:

$$\text{Moisture content (\%)} = \frac{(A - B)}{A} \times 100 \quad (7)$$

where  $A$  is the wet weight of brick and  $B$  is the dry weight of the brick.

### Loss on Ignition Test

A specimen mass of 160 g of each mix composition was placed in a furnace for approximately 10 min at 900°C and then cooled and reweighed. The process was repeated until a constant mass (no change in mass) was achieved. The loss on ignition of the raw material is roughly equivalent to the loss in mass that the bricks will undergo as furnace liners.

### Shatter Index Test

Kelson Shatter index tester (serial no. 7111; Kelsons Engineers and Fabricators, Maharashtra, India) is used to determine the bricks tendency to break in conventional transit and handling beyond the point of sampling. This method of drop shatter test covers the determination of the relative size

stability and its complement, the friability of the bricks, and the relative resistance to breakage of the bricks when handled in thin layers. A dried lump at room temperature (30°C) of 160 g of each blend was dropped several times from a height of 2 m onto a cast iron floor (0.5 × 0.5 × 0.03 m). Thereafter, the compositions were screened and the shatter index expressed as wt.% passing through a 5-mm sized screen was recorded.

### Refractoriness

Refractoriness points to the resistance of extreme conditions of heat (temperature > 1000°C). The refractoriness under load (RUL) test gives an indication of the temperature at which the bricks will collapse, in service conditions under similar load. Thirty different bricks were prepared, completely dried at room temperature (30°C), placed into a kiln, and fired to a temperature of 1200°C. Bricks with an ability to withstand exposure to elevated temperatures without undergoing deformation were noted, while others crumbled inside the kiln.

### Thermal Shock

The reversible thermal expansion is a reflection on the phase transformations that occur during heating and cooling. The bricks were placed into a furnace, heated at 900°C for 10 min, and removed from the kiln to cool in atmospheric air for another 10 min. This process was repeated 24 times, and the specimens with lower thermal expansion coefficient and less susceptible to thermal spalling were observed and noted.

### Thermal Conductivity

The mix composition brick's resistance per centimeter was recorded using a Myron L 512M5 analog conductivity meter. The resistivity of the composition was calculated, and the thermal conductivity was determined from this value.

### Permeability Test

An electric permeability meter model UM1-PERM (serial no 131/08-09) employed the orifice method and the pressure drop was indicated on a very sensitive gauge graduated directly in units. An expanding O-ring was used to form an airtight seal between the center post and the specimen tube, the required air pressure (10 cm of water) was supplied by a high-speed fan with rheostat-controlled universal motor, and the net readings were recorded. The dimensions of the sample were as follows: length = 115 mm, width = 56 mm, height = 12 mm, power supply = 110/115 V or 220/240 V, 1 phase, 50 and/or 60 Hz.

### Compressive Test

Compressive strength is the capacity of the bricks to withstand loads tending to reduce the size. The bricks are placed in a 5980 model floor model uni-

versal testing machine with over 53 MN capacities, compressed, and then shortened. The atomic level is forced together and the uniaxial compressive stresses reached when the bricks failed completely were observed and recorded.

### Scanning Electron Microscope (SEM)

An Aspek 3020 SEM, which uses a focused electron probe to extract structural and chemical information point-by-point from a region of interest in the sample, was used. The high spatial resolution of an SEM makes it a powerful tool to characterize a wide range of the sample at the nanometer to micrometer length scales.

## RESULTS AND DISCUSSION

After firing, the mixes with 500  $\mu\text{m}$  and 600  $\mu\text{m}$  size dross with 60, 65, and 70% aluminum dross crumbled. This suggests poor plastic mixture when the aluminum dross content is high making it hard for clay to bind. During the thermal shock test, more bricks are lost from the expansion and contraction that occurred in and out of the kiln, leaving the total brick left to 10 from a total of 30 consisting of mostly 150  $\mu\text{m}$  and 212  $\mu\text{m}$ . This result suggested that the finer the particles, the better its thermal stability.

### Shrinkage

#### Fire Shrinkage

The firing shrinkage of clay is a very useful and relevant property in the production of refractory bricks.<sup>16</sup> It is observed in Fig. 1 that increases in the fraction of aluminum dross in the refractory led to an increase in the fire shrinkage to a certain value before remaining constant with further addition. An exceptional case is noted for the refractory with 500- $\mu\text{m}$  sized Al dross where the fire resistance is independent of the weight fraction of the Al dross. The firing shrinkage is maximum at a higher weight fraction of the dross than at a low amount in all cases. Refractories with 70 wt.% of the Al dross possess the same shrinkage of 3.5% except that of 500- $\mu\text{m}$  sized Al dross, which shows a shrinkage of 2.0%. Ugheoke et al.<sup>17</sup> reported a maximum shrinkage of 13.6% for kaolin-rice husk refractory brick, showing that the use of Al dross inhibits the shrinkage of the clay refractory brick. This finding is in line with the study by Merzah et al.,<sup>18</sup> where alumina reduced the shrinkage of refractory bricks. In this case, it was noted that the presence of Al dross in small proportion reduces firing shrinkage, but higher shrinkage was observed with an increase weight fraction of the Al dross. This increase may be attributed to the presence of volatile matters in the Al dross.

#### Dry Shrinkage

Figure 2 shows the variation of drying shrinkage in relation to the weight fraction of Al dross for

different particle sizes. An overall decrease in the dry shrinkage was observed for all samples except for samples with 600- $\mu\text{m}$  sized Al dross with constant shrinkage. The drying shrinkage indicates to some degree the plasticity of the mixture. A large drying shrinkage means that mixture could absorb much water. The figure indicates that increase in weight fraction of Al dross promotes increase in the ability of the refractory material to absorb water. It is observed that 300- $\mu\text{m}$  sized Al dross-filled brick has the highest starting dry shrinkage. Bricks with 212, 150, and 425  $\mu\text{m}$  show the same starting dry shrinkage. It is also observed that all samples have the same dry shrinkage with 70 wt.% of the Al dross. This finding indicates that the presence of the Al dross is what favors the dry shrinkage of the bricks. Mohammed<sup>19</sup> recorded a decrease in dry shrinkage with an increase in weight fraction of grog filler in kaolin clay. However, the lowest dry shrinkage recorded in our study is approximately 65% higher than that observed by Mohammed.<sup>19</sup> This indicates the superiority of Al dross as raw material for bricks in terms of dry shrinkage.

### Apparent Porosity

The porosity of the refractory is expressed as average percentage of open pore space in the overall refractory volume. Highly porous materials tend to be highly insulating as a result of high volume of air trap in the brick because air is a very poor thermal conductor. As a result, low porous materials are generally used in hotter zones, whereas the more porous materials are usually used for thermal backup. Figure 3 shows that at 70 wt.% of 150- $\mu\text{m}$  sized Al dross has the highest apparent porosity (99.24%), whereas 40 wt.% 425  $\mu\text{m}$  Al dross has the lowest porosity (76.57%). The figure shows a general trend of similar porosity for all samples at all weight fraction of Al dross except for a few cases. The porosity of Al dross based bricks are high because the aluminum metal and other volatile matter content of the dross burns and pores are created in the brick, resulting in bricks that are better heat insulators; heat cannot pass through motionless air

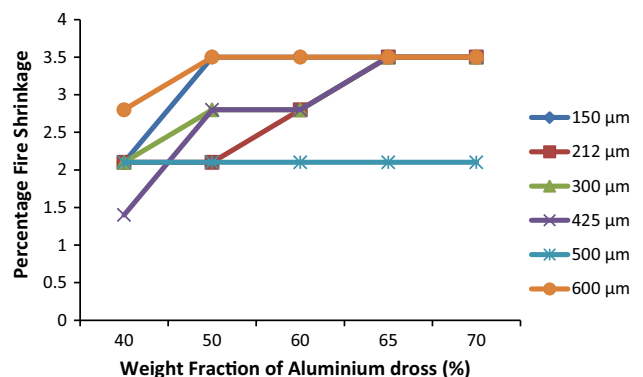


Fig. 1. Fire shrinkage responses of aluminum dross-kaolin blend bricks.

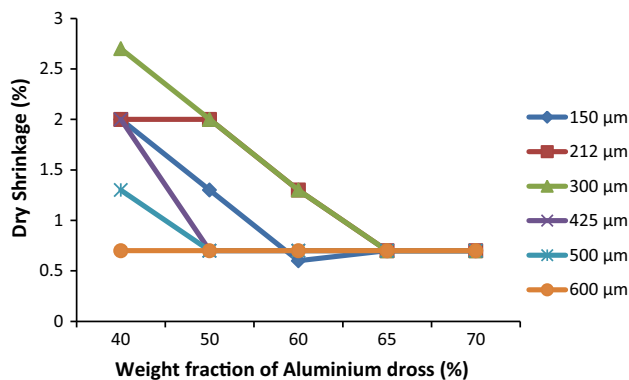


Fig. 2. Dry shrinkage responses of aluminum dross-kaolin blend bricks.

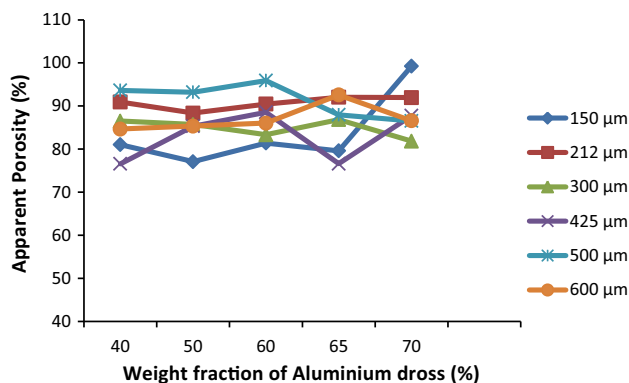


Fig. 3. Apparent porosity of aluminum dross-kaolin blend bricks.

trapped in the pores because they act as an insulator.<sup>20</sup> Ugheoke et al.<sup>17</sup> reported high porosity (95%) for rice-husk-filled clay bricks and attributed it to the burning of rice husk at the firing temperature. However, Mohammed<sup>19</sup> showed a decrease in porosity with increase on grog weight fraction in grog-kaolin bricks.

### Effective Moisture Content

In Fig. 4, there is an overall decrease in the moisture content of the bricks with increase in weight fraction of Al dross. This figure shows that the moisture content of the bricks is dependent on the weight percentage of aluminum dross. It is expected that Al dross does not absorb water because it contains water-resistant substances such as aluminum metal, alumina, and silica. At 70 wt.% fraction of Al dross, the bricks show higher moisture content for small particle-filled bricks compared with large particle-filled bricks.

### Dry Weight

Figure 5 shows the effect of weight fraction of Al dross and particle size on the dry weight of the formulated bricks. All samples exhibit similar dry

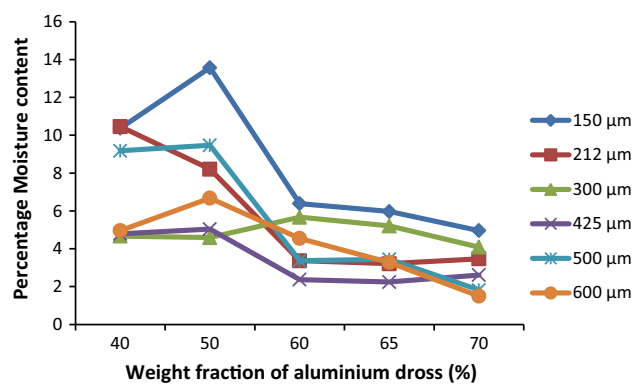


Fig. 4. Moisture content of aluminum dross-kaolin blend bricks.

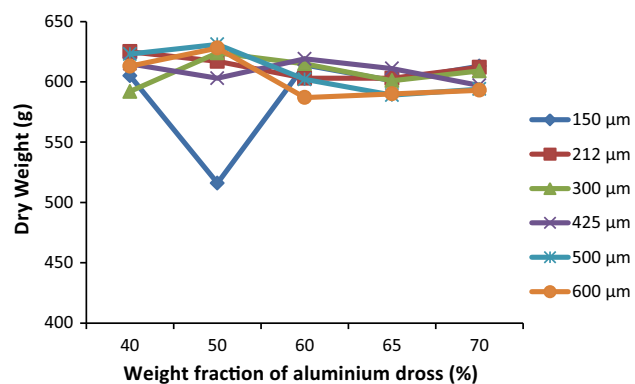


Fig. 5. Dry weight of aluminum dross-kaolin blend bricks.

weight with an increase in particle size and weight fraction of the Al dross additive. It is observed that the sample with 50 wt.% of 150- $\mu\text{m}$  Al dross brick has an unusual lowest dry weight of 516 g. It is also observed in Fig. 6 that this sample has the lowest wet weight. This unusual low weight might be attributed to its particle size and possibility of low water intake during the molding process. The sample with 50 wt.% of 500- $\mu\text{m}$  Al dross filler shows the highest dry weight of 631 g. Generally, it is observed that the dry weight of bricks decreases with an increase in weight fraction of the Al dross. This is an indication that the weight of the bricks is governed primarily by the content of kaolin, suggesting a reduction in weight with the use of Al dross. A maximum weight savings of 3% is observed in bricks with 600  $\mu\text{m}$  Al dross.

### Wet Weight

The as-fabricated weight of refractory bricks in relation with the weight fraction and particle size of Al dross is shown in Fig. 6. It is obvious that an increase in weight fraction of Al dross causes a decrease in the weight of bricks. This is an indication that the weight of the brick is determined by the clay content, suggesting that the use of Al dross led



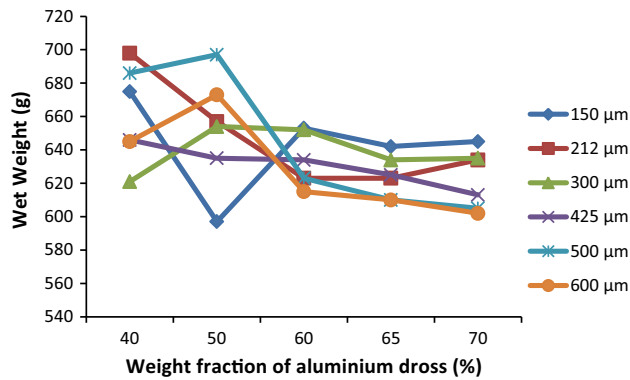


Fig. 6. Wet weight of aluminum dross-kaolin blend bricks.

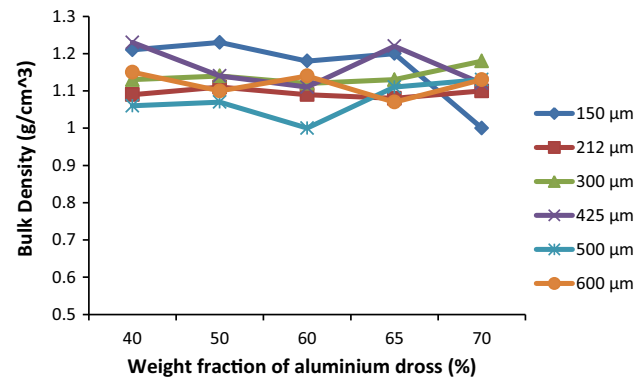


Fig. 8. Bulk density of aluminum dross-kaolin blend bricks.

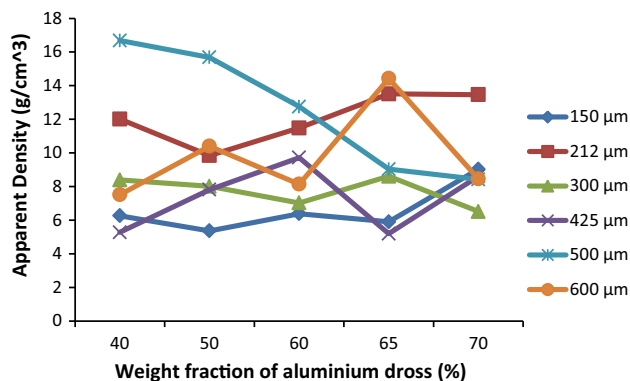


Fig. 7. Apparent density of aluminum dross-kaolin blend bricks.

to weight savings. It is also obvious from the figure that small particle-sized fillers have higher weights, whereas larger particle-sized fillers result in lower weights. The 40 wt.% 212- $\mu\text{m}$  Al dross brick has the highest wet weight (698 g), whereas the 50 wt.% 150- $\mu\text{m}$  Al dross brick with low water absorption shows the lowest wet weight of 597 g.

### Apparent Density

In Fig. 7, 40 wt.% 425- $\mu\text{m}$  Al dross brick possesses the lowest apparent density of  $5.27 \text{ g/cm}^3$ , whereas the 40 wt.% 500- $\mu\text{m}$  Al dross brick has the highest apparent density of  $16.68 \text{ g/cm}^3$ .

### Bulk Density

The bulk density is generally considered in conjunction with apparent porosity. It is a measure of the weight of a given volume of the refractory. For many refractories, the bulk density provides a general indication of the product quality. It is considered that the refractory with a higher bulk density (low porosity) will be better in quality. An increase in bulk density increases the volume stability, the heat capacity, as well as the resistance to abrasion and slag penetration. It is observed that the bulk

density of all formulations did not change considerably with an increase in weight fraction of Al dross (see Fig. 8). However, it is obvious that the introduction of Al dross led to a slight increase in bulk density for some samples but a decrease for some without a well-defined trend. Ugheoke et al.<sup>17</sup> observed a lower bulk density with rice husk filler, attributing it to the burning of rice husk during firing to create pores that lead to a decrease in density. Elngar et al.<sup>21</sup> also reported an increase in bulk density of the brick with a percentage of grog. In Fig. 8, 40 wt.% 425- $\mu\text{m}$  Al dross shows the highest bulk density of  $1.23 \text{ g/cm}^3$ , whereas the 60 wt.% 500- $\mu\text{m}$  Al dross brick has the lowest bulk density of  $1.00 \text{ g/cm}^3$ . The burning of ash and  $\text{K}_2\text{O}$  content of Al dross leaves pores in the sample, which reduces its density.

### Compressive Modulus

Figure 9 shows the variation of compressive modulus of bricks with increase in weight fraction of Al dross. All samples exhibit an initial rise in compressive modulus to a maximum value before a decline with further addition of the Al dross. All bricks show maximum modulus at 65 wt.% of Al dross except the sample with 455- $\mu\text{m}$  sized Al dross particles. The highest compressive modulus (233.0 MPa) is shown by bricks with 300- $\mu\text{m}$  sized Al dross at 65 wt.%, whereas the lowest is shown in bricks with 500  $\mu\text{m}$  at 70 wt.% Al dross (15.376 MPa).

### Permeability

Figure 10 shows the permeability of refractory bricks formulated with different weight fraction and particle sizes of Al dross. Permeability of the bricks is found to increase slightly with an increase in weight fraction of the Al dross for all samples, indicating that permeability is dependent on the Al dross. In the case of 600- $\mu\text{m}$  sized Al dross particles, permeability decreases initially with an increase in weight fraction of the Al dross, but later it increases to a maximum at 65 wt.% of the filler. The maxi-

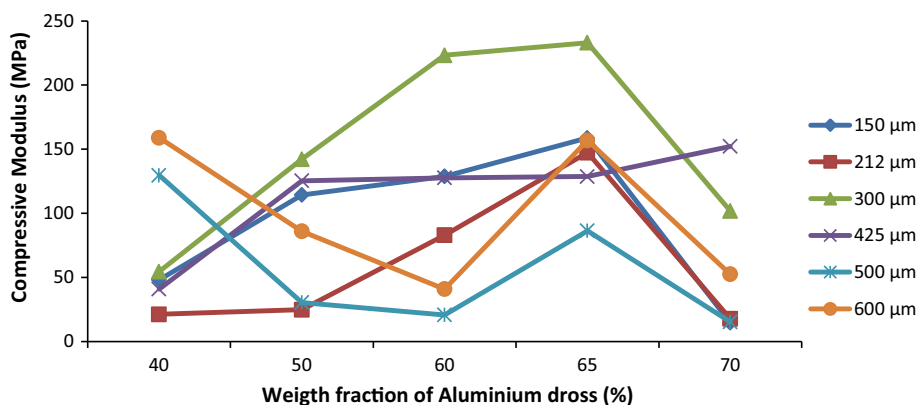


Fig. 9. Compressive modulus of aluminum dross-kaolin blend bricks.

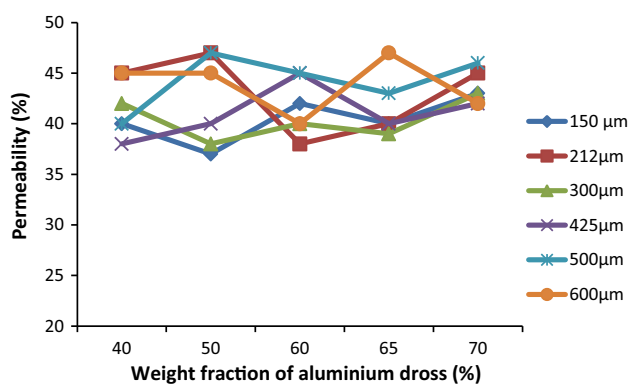


Fig. 10. Permeability of aluminum dross-kaolin blend bricks.

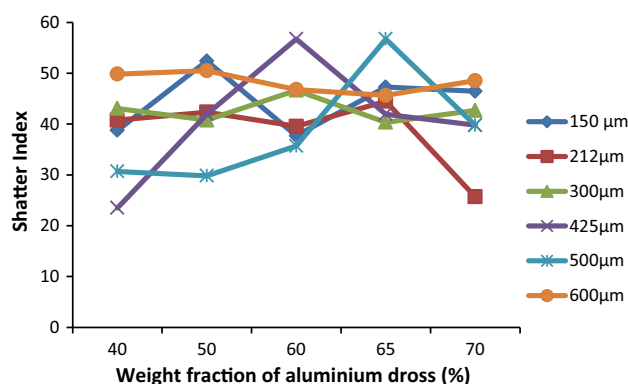


Fig. 11. Shatter index of aluminum dross-kaolin blend bricks.

imum permeability value (47%) is achieved with 600- $\mu\text{m}$  sized Al dross particles at 65 wt.%.

### Refractoriness

The results of refractoriness test confirm that samples consisting of 150  $\mu\text{m}$  and 212  $\mu\text{m}$  are all insulating firebricks that can withstand temperatures up to 1200°C. It is therefore proposed that they are of acceptable standard for hot-face insulating firebricks production.

### Thermal Conductivity

The results of thermal conductivity test indicate that all bricks possess thermal conductivities approximately equal to 0.358509  $\text{W m}^{-1} \text{K}^{-1}$ . This value is higher than that reported by Ugheoke et al.<sup>17</sup> and Folaranmi<sup>22</sup> for rice husk kaolin and saw dust clay bricks, indicating a superior thermal conductivity of the current bricks.

### Shatter Index

The shatter index is a measure of toughness of the bricks, particularly, the ability of brick to withstand rough handling and strain during handling. Figure 11 shows the variation of shatter index of the

bricks with an increase in weight fraction and particle size of the Al dross. The shatter index increases with an increase in weight fraction of the Al dross in the blend to a maximum for all samples except for samples with 300- $\mu\text{m}$  sized Al dross filled bricks where there is a gradual decline in the shatter index. The samples with 150-, 212-, 300-, 425-, 500-, and 600- $\mu\text{m}$  sized Al dross show maximum shatter index at 50, 65, 60, 60, 35, and 50 wt.%, respectively. The maximum shatter index (56.72) is shown by samples with 500- $\mu\text{m}$  sized Al dross at 65 wt.% followed by 425  $\mu\text{m}$  at 60 wt.%. The lowest shatter index (23.51) is shown by samples with 425- $\mu\text{m}$  sized Al dross at 40 wt.%. It is obvious from the preceding results that aluminum dross is responsible for the shatter index values.

### Loss on Ignition (LOI)

Figure 12 shows the effect of an increase in weight fraction of Al dross on the LOI of composite bricks. Bricks having 150- $\mu\text{m}$  sized dross possess high LOI at 40 wt.% of the Al dross, after which the LOI declines with an increase in the fraction of Al dross. Bricks with 600- $\mu\text{m}$  sized dross possess low LOI at 40 wt.% of the Al dross, after which the LOI increase gradually with an increase in the fraction

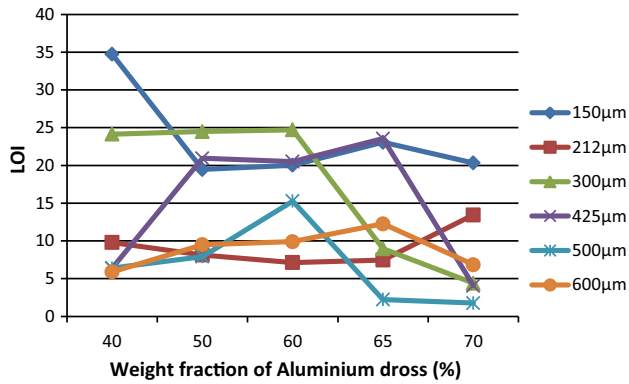


Fig. 12. Loss on ignition of aluminum dross-kaolin blend bricks.

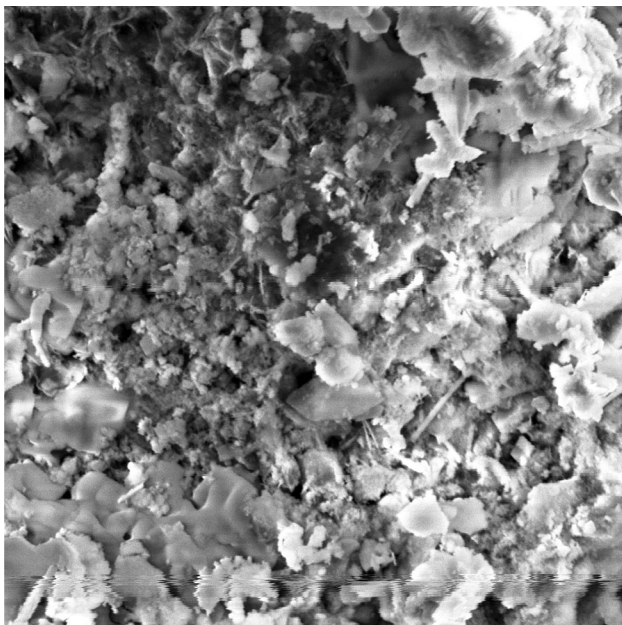


Fig. 13. SEM image of 150- $\mu\text{m}$  Al dross powder (2500 times).

of Al dross. Bricks with 300- $\mu\text{m}$  sized dross started with high LOI but declined continuously after 60 wt.% of the dross. On the other hand, bricks with 425- $\mu\text{m}$  sized dross started with low LOI and increased to a maximum at 65 wt.% of the dross, after which it declined to a minimum at 70 wt.%. Bricks with 500- $\mu\text{m}$  sized dross followed a similar trend. The lowest LOI (1.77%) is recorded for the brick with 70 wt.% of 500- $\mu\text{m}$  sized dross, whereas the highest LOI (34.75) is recorded for the brick with 40 wt.% 150- $\mu\text{m}$  sized dross.

### Scanning Electron Microscopy

Figure 13 shows the SEM image of 150  $\mu\text{m}$  aluminum dross. The image shows particles of the Al dross clung together having a complex mixture of all kinds of impurities. The particles appear nonuniform in size, probably indicating that it contains particles sizes less than 150  $\mu\text{m}$ . Figure 14 is the SEM image of

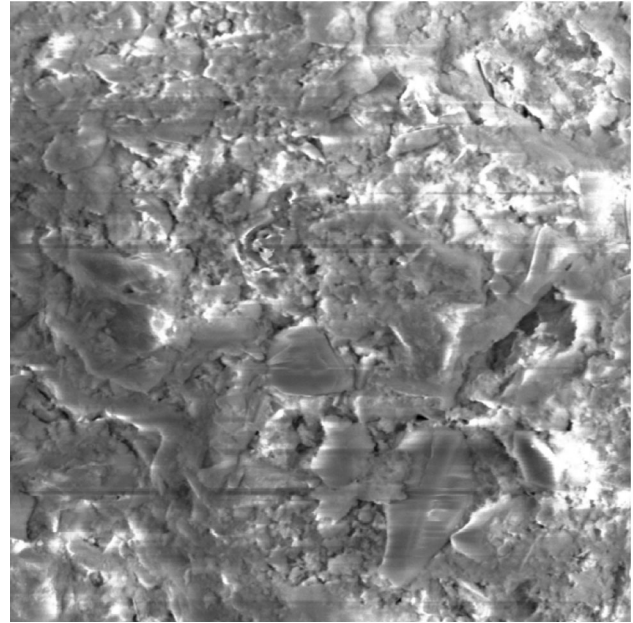


Fig. 14. SEM image of refractory brick with 150  $\mu\text{m}$  Al dross powder (2500 times).

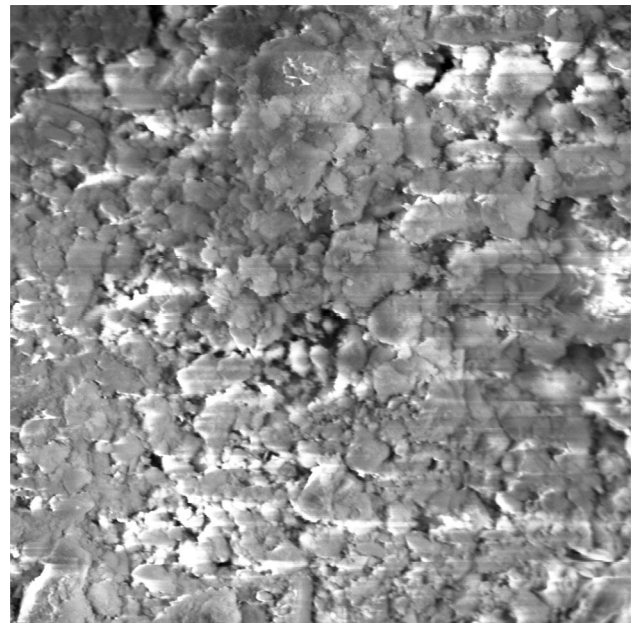


Fig. 15. SEM image of refractory brick with 500  $\mu\text{m}$  Al dross powder (2500 times).

refractory bricks containing 150- $\mu\text{m}$  sized Al dross powder. The image shows a good blend of the clay and dross with few voids appearing at some portions of the image. This is not the case with that of bricks containing 500  $\mu\text{m}$  Al dross (see Fig. 15) where the particles of Al dross and kaolin are observed clinging to each other and are not perfectly mixed, giving rise to large voids. The SEM images of the 150- $\mu\text{m}$  Al dross-filled brick show plastic morphology, whereas that of



500- $\mu\text{m}$  Al dross-filled brick show a porous morphology. The high porosity observed in the image of the 500- $\mu\text{m}$  Al dross-filled brick is probably the reason for the low compressive modulus and bulk density discussed in the previous sections. The image of the bricks containing 150- $\mu\text{m}$  sized Al dross powder also confirms the reason for high apparent porosity and low water adsorption and shrinkage of the brick discussed in previous sections.

### CONCLUSION

The results of this study have shown that aluminum dross, kaolin, and plastic clay are suitable for the production of insulating firebricks. Al dross bricks with 40–70 wt.% and particle sizes of 150  $\mu\text{m}$  and 212  $\mu\text{m}$  are the recommended sizes for insulating firebricks that can withstand temperatures up to 1200°C. They are of acceptable standard for hot-face insulating firebricks production. The 70 wt.% 150- $\mu\text{m}$  Al dross brick with porous structure is suitable for backup insulation. However, its composition can be varied to improve its refractoriness. The mixing ratio 65 wt.% Al dross bricks for sizes 300  $\mu\text{m}$  and 400  $\mu\text{m}$  have best combination of strength. These bricks will perform well when used as hot-face insulating firebricks and can serve as firebricks both for backup and hot-face insulation. For minimal effective moisture content, the cumulative weight percent of kaolin and clay (treated as a whole) in the brick must be about two thirds of the total weight of the firebrick.

### REFERENCES

1. W.E. Lee and R.E. Moore, *J. Am. Ceram. Soc.* 81, 1385 (1998).
2. Bricks from [www.bricks.com/documents](http://www.bricks.com/documents). Accessed 26 July 2013.
3. G.J. Kulik and J.C. Daley, *Second International Symposium—Recycling of Metals and Engineered Materials*, ed. Y. Sahai (Warrendale, PA: TMS, 1990), pp. 427–437.
4. D.L. Stewart, J.H.L.V. Linden, A.F. LaCamera, T.V. Pierce, J.O. Parkhill, J.M. Urbanic, and T.R. Hornack, U.S. patent 5057194 (1991).
5. S. Harris, *Ky. J. Equine, Agric. Nat. Resour. Law* 22, (2009). [www.kjeanrl.com/2009/09/fire-in-hole-aluminum-dross-in.html](http://www.kjeanrl.com/2009/09/fire-in-hole-aluminum-dross-in.html). Accessed 26 July 2013.
6. R. Breault, S.P. Tremblay, Y. Huard, and G. Mathieu, U.S. patent 5407459 (1995).
7. E.M.M. Ewais, N.M. Khalil, M.S. Amin, Y.M.Z. Ahmed, and M.A. Barakat, *Ceram. Int.* 35, 3381 (2009).
8. G. Chandrasekar, J. Kim, K.S. You, J.W. Ahn, K.W. Jun, and W.S. Ahn, *Korean J. Chem. Eng.* 26, 1389 (2009).
9. J.P. Hong, J. Wang, H.Y. Chen, B.D. Sun, J.J. Li, C. Chen, and T. Nonferr, *Metal. Soc.* 20, 2155 (2009).
10. H.N. Yoshimura, A.P. Abreu, A.L. Molisani, A.C. Camargo, J.C.S. Portela, and N.E. Narita, *Ceram. Int.* 34, 581 (2008).
11. M.N.I. Castro, J.M.A. Robles, D.A.C. Hernández, J.C.E. Bocardo, and J.T. Torres, *Ceram. Int.* 35, 921 (2009).
12. D. Chen, *J. Worcester Polytech. Inst.* 2, 40 (2012).
13. K.E. Lorber and H. Antrekowitsch, Institute for Sustainable Waste Management and Technology (IAE), Montan University Leoben, private communication, 2011.
14. E.D. Sehnke, *Proceedings of UNITECR* (São Paulo, Brazil: ALAFAR, 1993), pp. 658–670.
15. T.J. Carbone, *Alumina Chemicals: Science and Technology Handbook* (Westerville, OH: The American Ceramic Society, 1990), pp. 99–108.
16. A.A. Jock, F.A. Ayeni, L.S. Jongs, and N.S. Kangpe, *Int. J. Mater. Methods Tech.* 1, 189 (2013).
17. B.I. Ugheoke, E.O. Onche, O.N. Namessan, and G.A. Asikpo, *Leonardo Electron. J. Pract. Tech.* 9, 167 (2006).
18. A.S. Merzah, Y. Muhsin, and Y.K. Mahmood, *Eng. Tech. J.* 32, 953 (2014).
19. K.H. Mohammed, Babylon University, unpublished paper, [www.uobabylon.edu.iq/uobcoleges/filesshare/articles](http://www.uobabylon.edu.iq/uobcoleges/filesshare/articles). Accessed 26 July 2013.
20. H. Norsker, *The Self-Reliant Potter: Refractories and Kilns* (Friedr Braunschweig/Wiesbaden, Germany: Vieweg & Sohn, 1987).
21. M.A.G. Elngar, F.M. Mohamed, G. Asrar, M.S. Carmen, and M.E.H. Shalabi, *J. Ore Dress.* 11, 27 (2009).
22. J. Folaranmi, *AU J.T.*, 13, 53 (2009).